Journal of Information Systems Engineering and Management
2026, 11(1s)
e-ISSN: 2468-4376
https://www.jisem-journal.com/

Research Article

Optimization of different ETL and BSF Layers with defects Management for high-performance CIGS solar cells

Faycal Saidi[1,2], Idris Bouchama[2, 3], Moussa Merabet[1,2], Moufdi Hadjab[3,*], Selma Rabhi[4], Mouad Chettab[5], Mounir Bouras[3]

[1] *Electronics Department, Faculty of Technology, University of Setif 1, 19000, Algeria.*
[2] *Research Unit on Emerging Materials (RUEM), University Ferhat Abbas of Setif 1, Setif, 19000, Algeria.*
[3] *Electronics Department, Faculty of Technology, University of Msila, Msila, 28000, Algeria.*
[4] *Department of Chemistry, Laboratory of Innovative Environmental Preservation Techniques, Constantine 1 University, 25000, Algeria.*
[5] *Department of physics, Thin Films and Interfaces Laboratory, Constantine 1 University, 25000 Constantine, Algeria.*
Emails: moufdi.hadjab@univ-msila.dz .
** Corresponding Author Email: moufdi.hadjab@univ-msila.dz;*

ARTICLE INFO

Received: 05 Dec 2025
Revised: 20 Jan 2026
Accepted: 29 Jan 2026

ABSTRACT

In this work, we present a numerical investigation of the performance of CIGS based thin films solar cell by introducing different BSF and ETL materials. Employing SCAPS-1D simulation, we systemically analyzed the effects of the thickness, doping concentration Na and defects density (NT) of CIGS layer. The study revealed that the suitable incorporation of BSF and ETL was obtained for CBTS and SnSe2 respectively. The optimization of CIGS thickness from 0.2 µm to 1 µm, showed a critical influence on light absorption and carrier transport, with the efficiency rising from 25.66% to a peak value of 32.04%. However, beyond 1 µm, the PCE tends to stabilize and even slightly decrease, reaching 31.29% at 3.5 µm. Moreover, the increase in doping concentration Na in CIGS layer, particularly from 10^{12} cm-^{3} to 10^{18} cm-^{3} led to an increase in efficiency from 20.70% at low doping to 29.44% at 10^{18} cm-^{3}. The increasing of defects density in absorber layer led also to a significant degradation in the overall performance of the solar cell. Additionally, the results clearly demonstrated that the CIGS/CBTS and SnS2/CIGS interfaces must be carefully engineered to minimize interfacial defect states. Maintaining Nt below 10^{13} cm^{-3} is critical for preserving high Voc and overall device efficiency.

Keywords: CIGS, SCAPS-1D, Thin films, Efficiency, ETL layers, BSF layers, Solar cell.

INTRODUCTION

Thin-film CIGS (Copper Indium Gallium Selenide) solar cells have garnered significant interest due to their high absorption coefficient, tunable bandgap, and potential for high efficiency at reduced manufacturing cost (Zhu, L., et al., 2018). Despite these advantages, the overall performance of CIGS devices is highly sensitive to the choice and quality of Electron Transport Layers (ETLs) and Back Surface Field (BSF) layers, which influence charge separation, transport, and recombination dynamics (Zhu, L., et al., 2018; Tian, S.-S., et al. 2024; Monnaf, M. A., et al. 2025).

This study aims to investigate and optimize ETL and BSF material combinations to enhance the photovoltaic performance of CIGS solar cells. In particular, we evaluate several BSF materials (AgInTe2, CBTS, CuSbS2, CuSCN, MoSe2, Sb2S3, Sb2Se3) with four ETLs (CdS, SnS2, WS2, ZrS2), assessing their impact on key solar cell parameters: power conversion efficiency (PCE), short-circuit current density (Jsc), open-circuit voltage (Voc), and fill factor (FF). Further simulations explore the influence of absorber layer thickness, acceptor doping concentrations (NA), bulk defect densities (Nt), and interfacial defect states.[5]

The goal is to determine the most efficient and realistic CIGS solar cell configurations while identifying critical material and structural parameters that affect performance. This systematic approach offers insight into device physics and guides future experimental and fabrication efforts. We have performed a theoretical work by operating a simulation program called SCAPS 1-D (Solar Cell Capacitance Simulator structures one-dimension) software package to determine the photovoltaic parameters of the hetero-junction solar cells. This program is considered to

Journal of Information Systems Engineering and Management
2026, 11(1s)
e-ISSN: 2468-4376
https://www.jisem-journal.com/

Research Article

be a powerful tool to predict the performance of thin films based solar cells. This free tool was developed at ELIS, Gent University, Belgium and it is based on solving one dimension semiconductor basic equations (Poisson equation and continuity equation of electrons and holes) (Burgelman, M., et al. 2000).

METHODOLOGIES

Scaps-1d basic semiconductor equations

SCAPS-1D (Solar Cell Capacitance Simulator) is numerical simulation software used to model the electrical and optical behavior of thin-film solar cells. It solves the fundamental semiconductor equations, including the Poisson equation, continuity equations for electrons and holes, and transport equations. These equations describe the charge carrier distribution, recombination, and transport mechanisms within the device. They relate the electrostatic potential (ψ) to the charge density (ρ) (Tian, S.-S., et al. 2024; Burgelman, M., et al. 2000).

The Poisson equation, given by equation (1) (Bhattarai, S., et al., 2021):

$$\frac{\partial^2 \psi}{\partial x^2} = \frac{-\partial E}{\partial x} = \frac{\rho}{\epsilon_s} = \frac{-q}{\epsilon_s}\left(p - n + N_d^+ - N_a^- \pm N_{def}\right) \quad (1)$$

The continuity equations (2) and (3) for electrons and holes are expressed as:

Where n and p are the electron and hole densities, Jn and Jp are the respective current densities,[6]

$$-\frac{\partial J_p}{\partial x} + G - U_P(n, p) = 0 \quad (2)$$

$$-\frac{\partial J_n}{\partial x} + G - U_n(n, p) = 0 \quad (3)$$

G is the generation rate, and R is the recombination rate. SCAPS numerically solves these coupled equations using a discredited mesh, iterating until convergence is reached to obtain photovoltaic parameters such as Jsc, Voc, FF and efficiency. Here, J_p is the hole current density (A/m²), Jn is the electron current density (A/m²), q is the charge (C), μp and μn are the carrier mobilities (m²/Vs), E is the electric field (V/m), D_p and D_n are the Diffusion coefficients (m²/s), $\frac{\partial J_p}{\partial x}$ is the spatial gradient of the hole concentration (holes/m³/m), $\frac{\partial J_n}{\partial x}$ is the spatial gradient of the electron concentration (electrons/m³/m).

The hole current density and the electron current density can be expressed by the equations (4) and (5) (Bhattarai, S., & Das, T., 2021):

$$J_p = q\mu_p - qD_p\frac{\partial p}{\partial x} \quad (4)$$

$$J_n = q\mu_n - qD_n\frac{\partial p}{\partial x} \quad (5)$$

SCAPS-1D is a powerful one-dimensional solar cell simulation software developed by M. Burgelman at the Department of Electronics and Information Systems, University of Gents, Belgium. SCAPS-1D allows us to design solar cell structures and analyze their electrical properties and spectral response (Burgelman, M., et al., 2000). Moreover, it is capable of modeling multivalent defects and tunneling effects, which are commonly observed in thin-film heterojunction solar cells. SCAPS-1D is based on solving the basic carrier semiconductor equations using finite differentia.

Journal of Information Systems Engineering and Management
2026, 11(1s)
e-ISSN: 2468-4376
https://www.jisem-journal.com/

Research Article

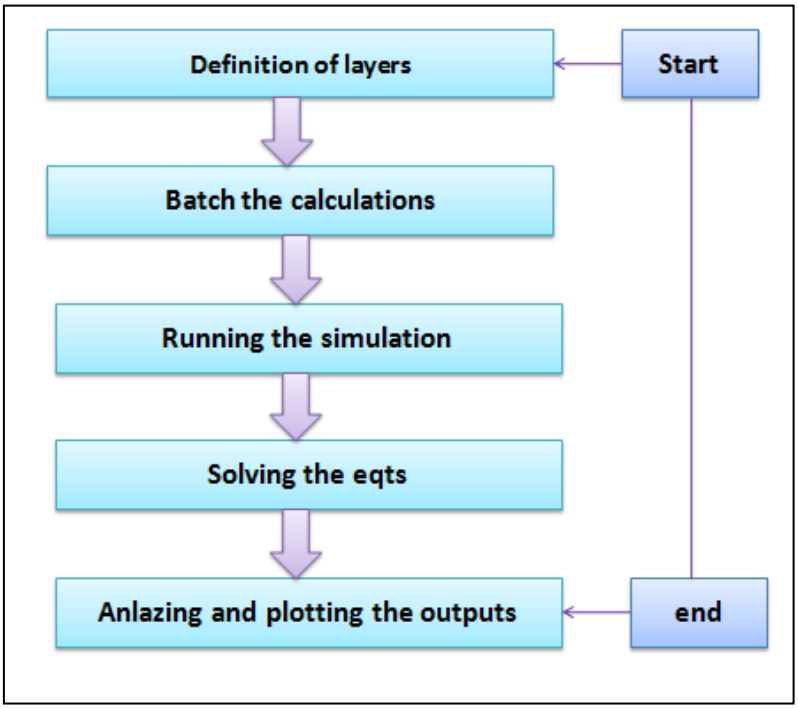

Figure 1: Steps for running the simulation in SCAPS-1D.

2.2 Structure and architecture's device

Cu(In,Ga)Se2 (CIGS) material is a semiconductor compound belonging to group I-III-VI, with a chalcopyrite crystal structure (Schock, H.-W., 1993). CIGS is promising for the development of high-performance photovoltaic applications in terms of stability and conversion efficiency (Oyedele, S. O., Soucase, B. M., & Aka, B., 2016). It is one of the main candidates to rival the efficiency and stability of conventional crystalline silicon cells, due to its high light absorption coefficient, lower material cost, and high stability (Valencia, D., et al., 2021). The limitation of its use is that CIGS integrates indium (In) and gallium (Ga), which are rare and expensive materials (Grandell, L., & Höök, M., 2015). The amount of these materials in the CIGS cell can be reduced by optimizing the thickness of the absorber (Chadel, M., et al., 2023).

Recent advancements in CIGS solar cell efficiency have been demonstrated through innovative back surface field (BSF) materials. For example, Ferdous Rahman et al. presents the exceptional performance of (CIGS)-based double hetero-junction (DH) photovoltaic cell (Rahman, M. F., et al., 2024). A novel solar cell structure (FTO/SnS2/CIGS/Sb2S3/Ni) is proposed and analyzed using SCAPS-1D simulation software to optimize key performance parameters. The research explores the effects of varying the thickness of the buffer, absorber, and back surface field (BSF) layers, as well as factors like acceptor and defect densities, capacitance–voltage (C-V) characteristics, interface defect density, generation and recombination rates, operating temperature, current density, and quantum efficiency. Comparisons are made between devices with and without the BSF layer. The BSF significantly enhances device performance, including short-circuits current density (Jsc), open-circuit voltage (Voc), fill factor (FF), and power conversion efficiency (PCE). After optimization, the conventional CIGS cell structure (FTO/SnS2/CIGS/Ni) achieved a PCE of 22.14%, with a Voc of 0.91 V, Jsc of 28.21 mA/cm², and FF of 86.31%. By integrating a Sb2S3 BSF layer, the PCE was notably improved to 31.15%, with a Voc of 1.08 V, Jsc of 33.75 mA/cm², and FF of 88.50%. These findings demonstrate that the proposed CIGS-based DH solar cells provide a promising pathway to higher efficiency, outperforming traditional designs.

In this study, we simulated the work of Rahman et al., who previously demonstrated the effectiveness of a novel BSF material in enhancing the efficiency of CIGS solar cells. By replicating their setup and optimizing similar

Journal of Information Systems Engineering and Management
2026, 11(1s)
e-ISSN: 2468-4376
https://www.jisem-journal.com/

Research Article

parameters in SCAPS-1D, we obtained results consistent with their reported values for power conversion efficiency, open-circuit voltage, and fill factor. These comparable results validate the reliability of our simulation approach and provide a solid foundation for further research. Building upon the endpoint of Rahman et al.'s study, we aim to explore additional modifications to the BSF and ETL layers to achieve even greater efficiency in CIGS devices.

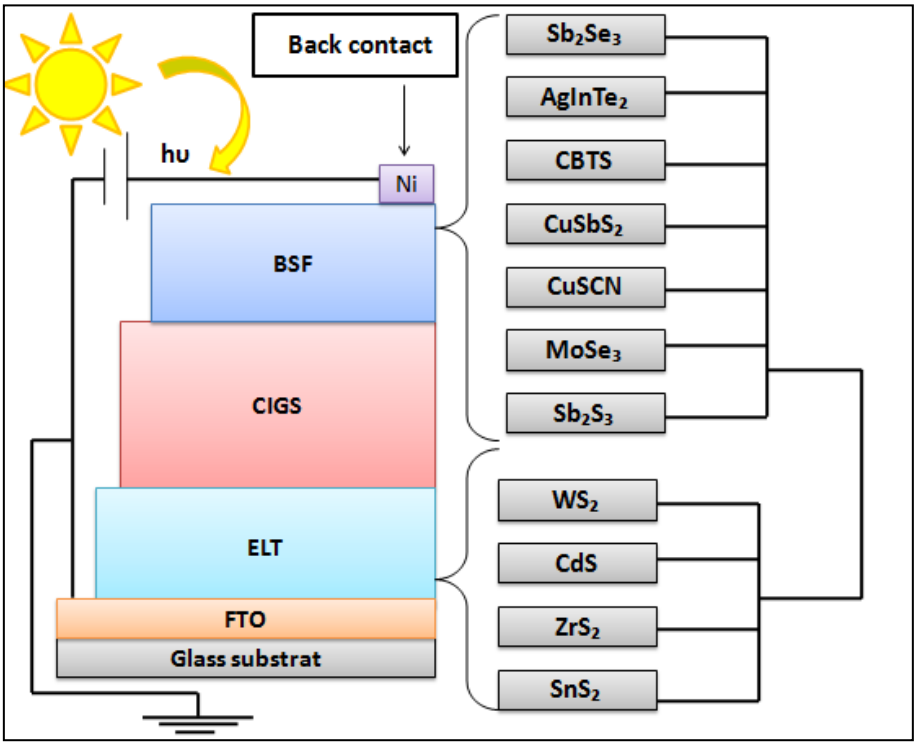

Figure 2: Illustration for the suggested cell device with different ETL/BSF layers

Table 1: Physical parameters and defect state for materials used in the simulation

Parameter	FTO	CIGS	ETL Layers			
			SnS2	ZrS2	CdS	WS2
Thickness (mm)	0.05	0.5*	0.05	0.05	0.1	0.05
Bandgap (eV)	3.6	1.1	2.24	2.5	2.45	1.8
Electron affinity (eV)	4	4.2	4.24	4.1	4.45	3.95
Dielectric permittivity (relative)	9	13.6	10	16.4	10	13.6
CB effective DOS (cm^{-3})	2.2×10^{18}	2.2×10^{18}	2.2×10^{18}	2.2×10^{18}	2.0×10^{18}	$1x10^{17}$
VB effective DOS (cm^{-3})	1.8×10^{19}	1.8×10^{19}	1.8×10^{19}	1.8×10^{19}	1.5×10^{19}	$2.4x10^{16}$
Electron mobility ($cm^2\ V^{-1}\ s^{-1}$)	100	100	50	$2.3x10^3$	50	100
Hole mobility ($cm^2\ V^{-1}\ s^{-1}$)	25	25	50	$1.3x10^3$	20	100
Donor density, ND	$1x10^8$	0	$1x10^{15}$	$1x10^{15}$	$1x10^{15}$	$1x10^{18}$

Journal of Information Systems Engineering and Management
2026, 11(1s)
e-ISSN: 2468-4376
https://www.jisem-journal.com/

Research Article

(cm-3)						
Acceptor density, NA (cm-3)	0	1x10^15*	0	0	0	0
(*) variable field						

Parameter	BSF Layers						
	Sb2Se3	AgInTe2	CBTS	CuSbS2	CuSCN	MoSe2	Sb2S3
Thickness (mm)	0.02	0.5	0.2	0.2	0.35	0.4	0.2
Bandgap (eV)	1.06	1.16	1.9	1.5	3.4	1.1	1.62
Electron affinity (eV)	4.15	3.6	3.6	4.2	1.9	4.14	3.7
Dielectric permittivity (relative)	19	8.9	5.4	14.6	10	13.6	7.08
CB effective DOS (cm-3)	1x10^18	3.66x10^19	2.2×10^18	2×10^18	1.7×10^17	2.2 × 10^18	2×10^19
VB effective DOS (cm-3)	1.8x10^20	1.35x10^19	1.8×10^19	1×10^18	2.5×10^19	1.8 × 10^19	1×10^19
Electron mobility (cm2 V-1 s-1)	10	1011	30	49	0.0001	100	9.8
Hole mobility (cm2 V-1 s-1)	1	887	10	49	0.1	25	10
Donor density, ND (cm-3)	0	0	0	0	0	0	0
Acceptor density, NA (cm-3)	1x10^14	3.5x10^19	1 × 10^15	1×10^18	1.1×10^18	1× 10^16	1×10^15

RESULTS AND DISCUSSIONS

Optimized analysis of etl and bsf combinations for cigs solar cells structures

According the **Table 2**, the simulation results highlight the significant impact of different ETL and BSF materials on the performance of CIGS solar cells. Among the tested configurations, SnS2 with CBTS, Sb_2S_3, CuSCN, or $MoSe_2$ achieved the highest power conversion efficiency (31.44%), closely followed by ZrS2 with CBTS, $Sb2S_3$, CuSCN, or MoSe2, which reached 31.43%. In terms of short-circuit current density (Jsc), SnS2/CBTS exhibited the highest value at 43.738 mA/cm², indicating superior charge collection efficiency. Meanwhile, the highest open-circuit voltage (Voc) was recorded in ZrS2 paired with AgInTe2 or Sb2S3, reaching 0.9340 V, which reflects a strong built-in potential and minimal recombination losses. Additionally, the highest fill factor (FF) was observed in SnS2/MoSe2 at 80.05%, suggesting enhanced charge transport properties. Overall, SnS2/CBTS emerges as the most optimal configuration, striking a balance between efficiency, high current density, and competitive voltage output, making it a strong candidate for further performance enhancements in CIGS solar cells.

To further refine the selection of the best-performing configurations, a comparative analysis was conducted to identify the most promising ETL and BSF combinations. By evaluating key performance parameters such as efficiency, short-circuit current density, open-circuit voltage, and fill factor, the two top-performing configurations were determined. This focused assessment provides a more precise understanding of the materials that offer the best balance between charge collection efficiency, built-in potential, and overall device performance. Among the tested configurations, the two most promising solar cell combinations are SnS2 as the ETL with CBTS as the BSF and ZrS2 as the ETL with CBTS as the BSF. The SnS2/CBTS combination demonstrates the highest efficiency

Journal of Information Systems Engineering and Management
2026, 11(1s)
e-ISSN: 2468-4376
https://www.jisem-journal.com/

Research Article

(31.44%), along with an excellent short-circuit current density (43.738 mA/cm²), a strong open-circuit voltage (0.9319 V), and a competitive fill factor (77.12%), making it the most effective in charge collection. On the other hand, the ZrS2/CBTS configuration closely follows with a 31.43% efficiency, a slightly higher open-circuit voltage (0.9340 V), a short-circuit current density of 43.729 mA/cm², and a fill factor of 76.96%, highlighting its strong built-in potential and low recombination losses. Both configurations offer an optimal balance of efficiency, current density, voltage, and charge transport properties, making them excellent candidates for further optimization and experimental validation in advancing CIGS solar cell technology.

Table 2 : The photovoltaic parameters (PCE, FF, Jsc and Voc) with different BSF and ETL

	BSF	AgInTe2	CBTS	CuSbS2	CuSCN	MoSe2	Sb2S3	Sb2Se3
ETL								
CdS	PCE (%)	25.03	27.13	27.01	27.13	27.04	27.13	25.25
	FF (%)	78.65	78.75	78.39	78.76	78.76	78.76	78.79
	J_{sc} (mA/cm²)	41.31215	43.734	43.734	43.733	43.62194	43.733	41.468
	V_{oc} (V)	0.7702	0.7878	0.7878	0.7878	0.7869	0.7878	0.7728
SnS_2	PCE (%)	26.09	31.44	31.31	31.43	30.56	31.44	26.37
	FF (%)	79.82	77.12	77.51	77.15	80.05	77.13	79.62
	J_{sc} (mA/cm²)	41.31009	43.738	43.738	43.738	43.62642	43.738	41.466
	V_{oc} (V)	0.7913	0.9319	0.9236	0.9316	0.8749	0.9319	0.7987
WS_2	PCE (%)	19.56	19.56	19.52	19.54	15.55	19.55	4.65
	FF (%)	50.05	50.05	50.24	50.01	43.73	50.03	27.82
	J_{sc} (mA/cm²)	40.46058	40.460	40.445	40.452	38.60775	40.457	19.868
	V_{oc} (V)	0.9661	0.9661	0.9608	0.9658	0.9208	0.9660	0.8415
ZrS_2	PCE (%)	25.53	31.43	31.31	31.43	30.52	31.43	25.84
	FF (%)	78.88	76.96	77.36	76.99	79.94	76.96	78.75
	J_{sc} (mA/cm²)	40.90534	43.728	43.728	43.728	43.59697	43.728	41.087
	V_{oc} (V)	0.7913	0.9340	0.9254	0.9336	0.8756	0.9340	0.7987

Journal of Information Systems Engineering and Management
2026, 11(1s)
e-ISSN: 2468-4376
https://www.jisem-journal.com/

Research Article

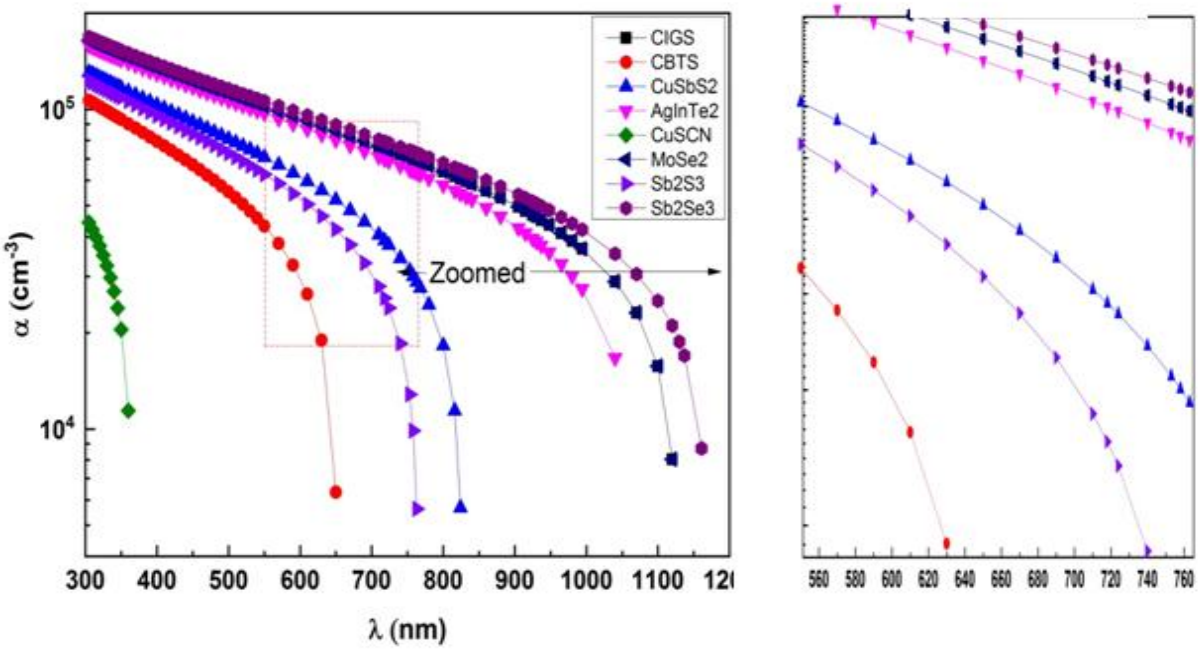

Figure 3: The absorption coefficients of different BSF layers.

The **Figure 3** shows that the absorption coefficient (α) as a function of wavelength plays a critical role in evaluating the optical compatibility of back surface field (BSF) layers with the CIGS absorber. The provided dataset compares the spectral absorption behavior of several candidate BSF materials including CBTS, CuSbS2, AgInTe2, CuSCN, MoSe2, Sb2S3, and Sb2Se3 against that of the CIGS layer. Among these, Sb2Se3 and Sb2S3 exhibit high absorption coefficients across a wide spectral range, particularly extending well into the near-infrared region, which suggests strong light-harvesting potential. However, their relatively high absorption at longer wavelengths could also lead to unwanted photon losses at the rear interface due to parasitic absorption, which is not always favorable in a BSF layer. In contrast, CBTS shows a more gradual and uniform decrease in absorption with increasing wavelength. Notably, its spectral behavior aligns well with CIGS, especially in the 600–900 nm range, where solar irradiance remains significant. This optical matching is essential to ensure minimal losses due to spectral mismatch, enabling better reflection of unabsorbed photons back toward the absorber layer (Meusel, M., et al., 2002; Seaman, C. H., 1982).

While CBTS does not exhibit the highest absolute absorption values, its moderate absorption coupled with a smooth spectral response can reduce rear recombination and enhance internal reflection. Moreover, CBTS has a distinct advantage in terms of material sustainability: it consists of earth-abundant, non-toxic elements, making it attractive for scalable and environmentally friendly solar technologies (Oublal, E., et al., 2022; Djatoubai, E., & Su, J., 2021). On the other hand, materials like MoSe2 and AgInTe2 display relatively lower absorption in the critical visible and near-infrared regions, which might limit their effectiveness in photon recycling when used as BSF layers. Although Sb2Se3 outperforms CBTS in terms of pure absorption magnitude, CBTS offers a more balanced optical profile with better spectral matching to CIGS. Combined with its benign environmental footprint and potential for improved carrier selectivity, CBTS emerges as a promising BSF candidate, especially in applications where material compatibility and long-term stability are prioritized over maximum absorption.

Effect of Absorber Layer CIGS Thickness on Solar Cell Performance

The results indicate a clear enhancement in the power conversion efficiency (PCE) as the absorber thickness increases from 0.2 μm to 1 μm, with the efficiency rising from 25.66% to a peak value of 32.04%. This improvement

Journal of Information Systems Engineering and Management
2026, 11(1s)
e-ISSN: 2468-4376
https://www.jisem-journal.com/

Research Article

can be attributed to the increased ability of thicker absorber layers to capture more incident photons, which enhances electron-hole pair generation and increases the short-circuit current density (Isc). The Increased light absorption generates more electron-hole pairs, leading to a higher Jsc. It can increase the probability of charge carrier separation and reduce recombination losses. However, beyond 1 µm, the PCE tends to stabilize and even slightly decrease, reaching 31.29% at 3.5 µm.

This behavior is likely due to the absorber approaching optical saturation, where additional thickness contributes little to light absorption while increasing recombination losses and reducing the open-circuit voltage (Voc). Moreover, the thicker absorber layer leads to an increase in cell resistance and diffusion length, which causes severe unwelcomed recombination of photogenerated carriers. Looking at the Voc trend, it decreases gradually with increasing thickness from 2.1158 V at 0.2 µm down to 0.9151 V at 3.5 µm.

.

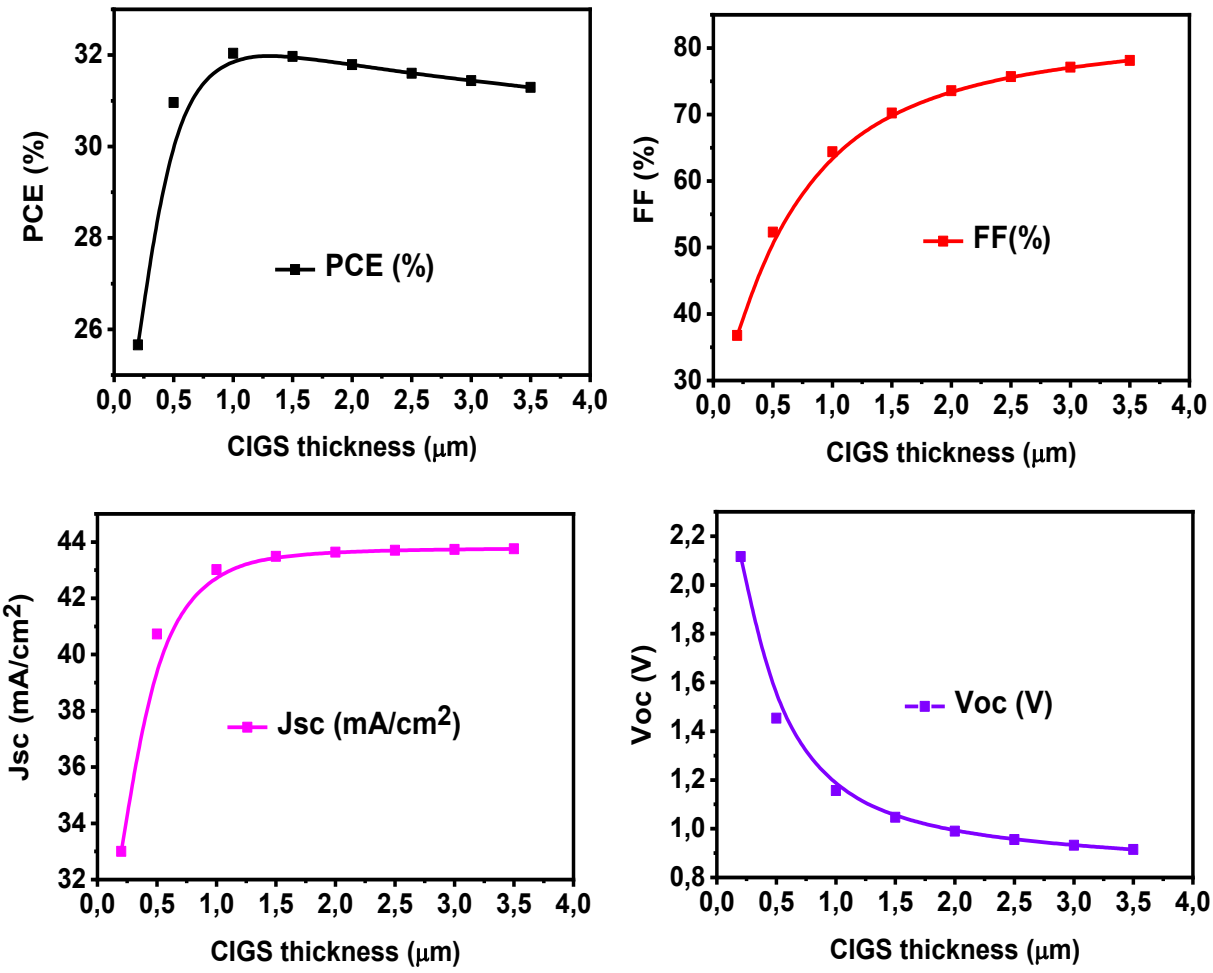

Figure 4: The influence of varying the absorber layer thickness on the photovoltaic performance of the CIGS solar cell with a BSF layer, under a constant temperature of 300 K.

This reduction can be linked to enhanced recombination and potential degradation in the built-in electric field in thicker layers. Meanwhile, the short circuit current (Isc) increases steadily with thickness, reaching a near-saturation value of about 43.76 mA, indicate a partial saturation of light absorption. The fill factor (FF) shows a significant increase with absorber thickness, improving from 36.76% to 78.14%. This suggests improved diode quality and reduced series resistance, contributing positively to the overall performance (Del Cueto, J., 1998; Del

Journal of Information Systems Engineering and Management
2026, 11(1s)
e-ISSN: 2468-4376
https://www.jisem-journal.com/

Research Article

Cueto, J., 1999). Based on these results, an absorber thickness of 1 μm is considered optimal, offering a balanced trade-off between V_{oc}, I_{sc}, and FF, and achieving the highest recorded efficiency of 32.04%.

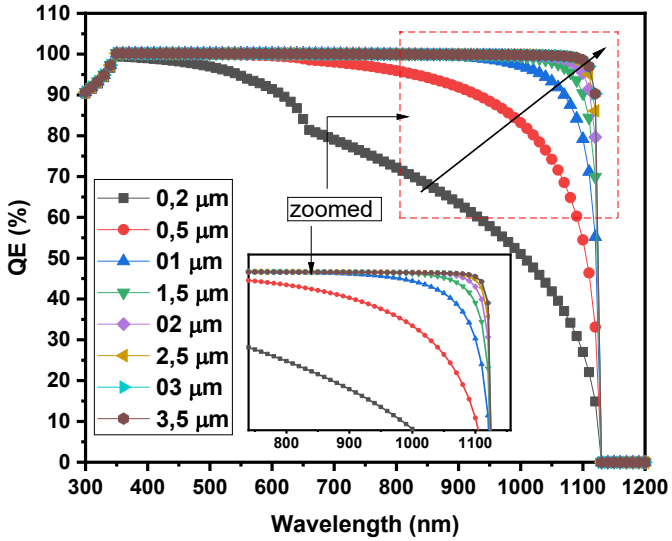

Figure 5: Variation of quantum efficiency with increasing of thickness CIGS layer

Effect of Acceptor Doping Concentration of CIGS Absorber Layer

As observed, the power conversion efficiency (PCE) shows a consistent improvement with the increase in doping concentration, particularly from 10^{12} cm-3 to 10^{18} cm-3. The efficiency increases from 20.70% at low doping to 29.44% at 10^{18} cm-3. This trend is primarily attributed to better charge carrier separation and an enhancement in the built-in electric field within the absorber, which reduces recombination losses (Sylla, A., et al., 2021).

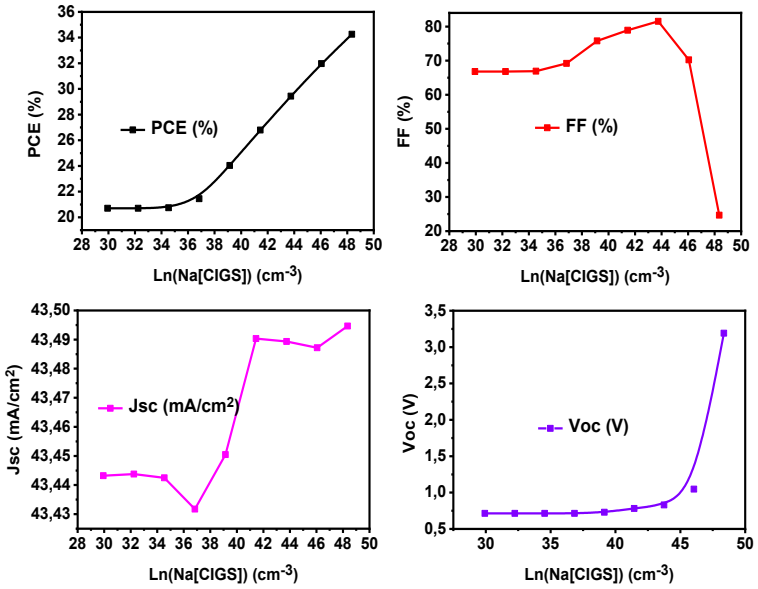

Figure 6: Demonstrates the influence of varying the acceptor doping concentration (NA) of the CIGS absorber layer on key photovoltaic parameters.

Journal of Information Systems Engineering and Management
2026, 11(1s)
e-ISSN: 2468-4376
https://www.jisem-journal.com/

Research Article

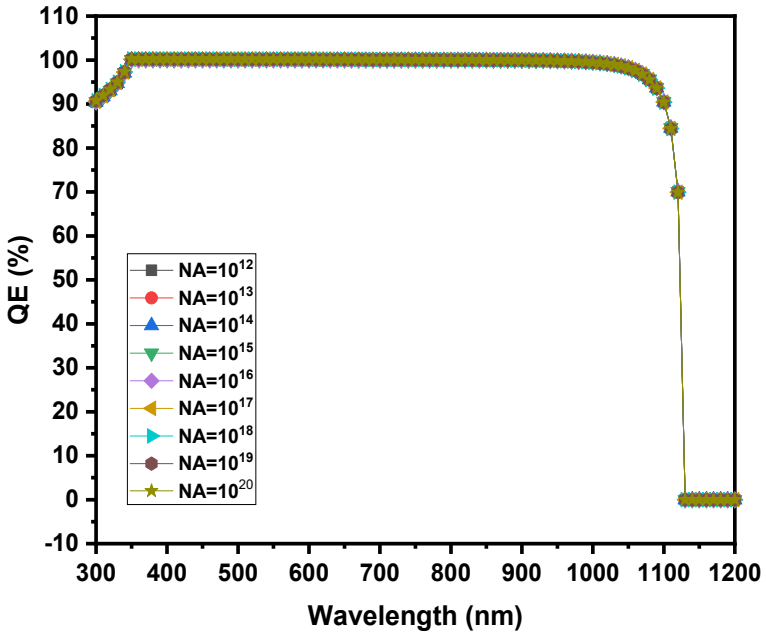

Figure 7: Variation of quantum efficiency with increasing of acceptor doping in CIGS layer.

The strategic introduction of n-type or p-type dopants, a process known as doping, serves to enhance the cells' photovoltaic efficiency by fine-tuning charge transport and carrier density, thereby optimizing device performance (Asaduzzaman, et al., 2016). The fill factor (FF) follows a similar trend, increasing from 66.80% to 81.53% within the same doping range, indicating an improvement in diode quality and reduced series resistance (Del Cueto, J., 1998; Del Cueto, J., 1999). Meanwhile, the short-circuit current density (Isc) remains relatively stable across all doping levels, with values around 43.44 mA/cm², suggesting that doping concentration has minimal influence on light absorption under the tested conditions. A notable increase is observed in the open-circuit voltage (Voc), which rises from 0.7133 V at 1012 cm-³ to 0.8305 V at 10^{18} cm-³. This increase is associated with enhanced band bending and reduced recombination at higher doping levels, leading to a higher built-in potential (Ghavami, F., & Salehi, A., 2020; Kamikawa, Y., et al., 2025).

However, beyond the optimal doping point of 10^{18} cm-³, performance degrades sharply. At 10^{19} cm-³, despite a higher Voc of 1.0469 V, the FF drops to 70.23%, and at 1020 cm-³, although Voc peaks at 3.1905 V, the FF collapses to 24.69% and overall efficiency declines. This degradation may result from excessive doping, which introduces deep-level defects and increases recombination via Auger processes or field screening effects (Benchiheb, N., et al., 2024). Based on these observations, an acceptor doping concentration of 10^{18} cm-³ is considered optimal for maximizing solar cell efficiency, balancing all performance parameters effectively.

Journal of Information Systems Engineering and Management
2026, 11(1s)
e-ISSN: 2468-4376
https://www.jisem-journal.com/

Research Article

Effect of Defect Density (Nt) of CIGS Absorber Layer on Device Performance

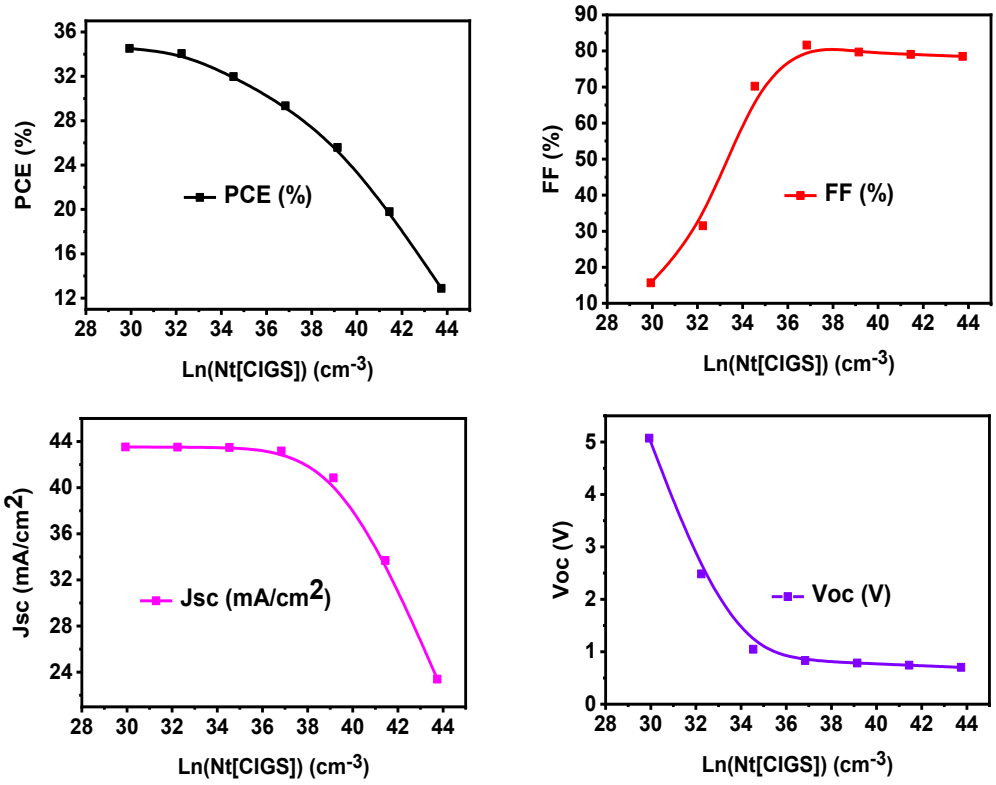

Figure 8: Presents the effect of varying the defect density (Nt) in the CIGS absorber layer on the photovoltaic parameters of the solar cell. The Nt values range from 10^{12} cm^{-3} to 10^{18} cm^{-3}

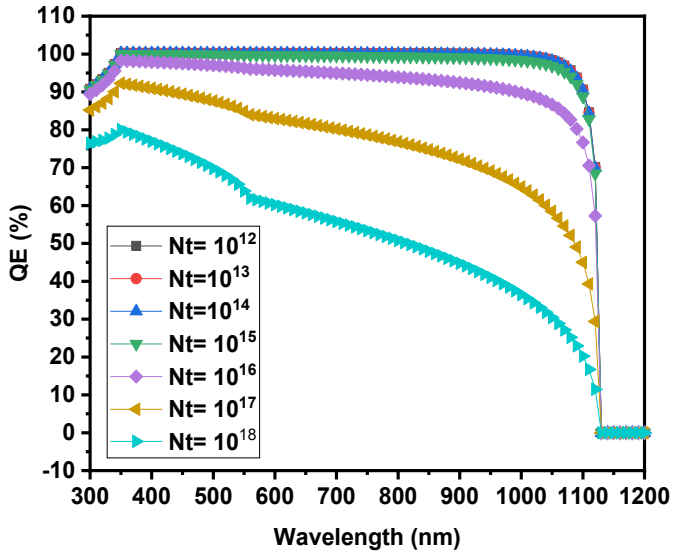

Figure 9: Variation of quantum efficiency with increasing of defects density of CIGS layer.

Journal of Information Systems Engineering and Management
2026, 11(1s)
e-ISSN: 2468-4376
https://www.jisem-journal.com/

Research Article

As shown in the results, increasing the defect density leads to a significant degradation in the overall performance of the solar cell. At low defect levels (10^{12} cm^{-3}), the device exhibits a very high open-circuit voltage (Voc) of 5.0714 V, though with a very low fill factor (FF) of 15.64%, indicating a highly non-ideal diode behavior. This unusual Voc value is likely an artifact of simulation at extremely low defect levels where recombination is nearly negligible. As Nt increases to 10^{13} cm^{-3} and 10^{14} cm^{-3}, a sharp drop in Voc is observed from 5.0714 V down to 1.0469 V accompanied by a considerable rise in FF, reaching 70.23% at 10^{14} cm^{-3}. This transition suggests that the device enters a more realistic operating regime where recombination becomes significant and balances the charge transport, resulting in more stable parameters. Beyond this point, continued increases in defect density have a clearly detrimental effect. At Nt values above 10^{14} cm^{-3}, Voc continues to decrease steadily, reaching 0.7012 V at 10^{18} cm^{-3}. Simultaneously, Isc and PCE also decline, with Isc dropping from 43.5 mA/cm^2 to 23.4 mA/cm^2 and PCE falling from 31.97% at 1014 cm^{-3} to just 12.88% at 10^{18} cm^{-3}. This performance degradation is directly related to the increase in recombination centers within the absorber. Higher Nt introduces more trap states that facilitate non-radiative recombination, reducing both carrier lifetime and diffusion length, thereby lowering Voc, Isc, and overall efficiency. This decreasing in PV parameters with increasing of Nt can explained by the decline in diffusion time $\boldsymbol{\tau}$n and $\boldsymbol{\tau}$p with the increasing of Nt in active layer which facilities the trapping of charges in these defects. Moreover, elevated Nt values can cause a narrowing of the spectral bandwidth and a significant drop in peak responsively, indicating a loss of effective photo response and charge extraction (Dimitrijev, S., 2006). These findings emphasize the critical importance of maintaining low defect densities in the absorber material to ensure optimal solar cell performance. The optimal Nt value, based on this data, appears to be in the order of 10^{14} cm^{-3}, balancing a realistic Voc and high FF and efficiency.

Table 3: Impact of defect density on length diffusion (Ln, Lp) and time of recombination ($\boldsymbol{\tau}$n, $\boldsymbol{\tau}$p).

Nt	Ln (μm)	Lp (μm)	τn (ns)	τp (ns)
10^{12}	160	80	10^5	10^5
10^{13}	51	25	10^4	10^4
10^{14}	16	8	10^3	10^3
10^{15}	5.1	2.5	10^2	10^2
10^{16}	1.6	0.8	10	10
10^{17}	0.51	0.25	1	1
10^{18}	0.16	0.08	0.1	0.1

Effect of Interfacial Defect Density at the SnS2/CIGS Interface on Solar Cell Performance

The interface between the layers in general plays a very crucial role in the performance of the device. If the interface has greater defects, greater will the recombination and loss of carriers, and thereby, decreasing the efficiency of the device (Cheng, S., 2024). The influence of the interface defects can be seen in following equation (6):

$$v_{oc} = \frac{1}{q}\left(\Phi_c + AK\,\mathrm{Ln}\left(\frac{q\,N_v S_{it}}{J_{sc}}\right)\right) \qquad (6)$$

where Sit is the interface recombination velocity, A is the ideality factor, and Φc is the effective barrier height. High interface defects will lead to a low Voc. All the photovoltaic parameters declined rapidly with the increase in defect density. The parameters decreased drastically till the defect density became 10^{18} cm^{-3}, and then it remained the same. Both the results indicate that the defect density influences the recombination rates, lifetime, and mobility of carriers.

Journal of Information Systems Engineering and Management
2026, 11(1s)
e-ISSN: 2468-4376
https://www.jisem-journal.com/

Research Article

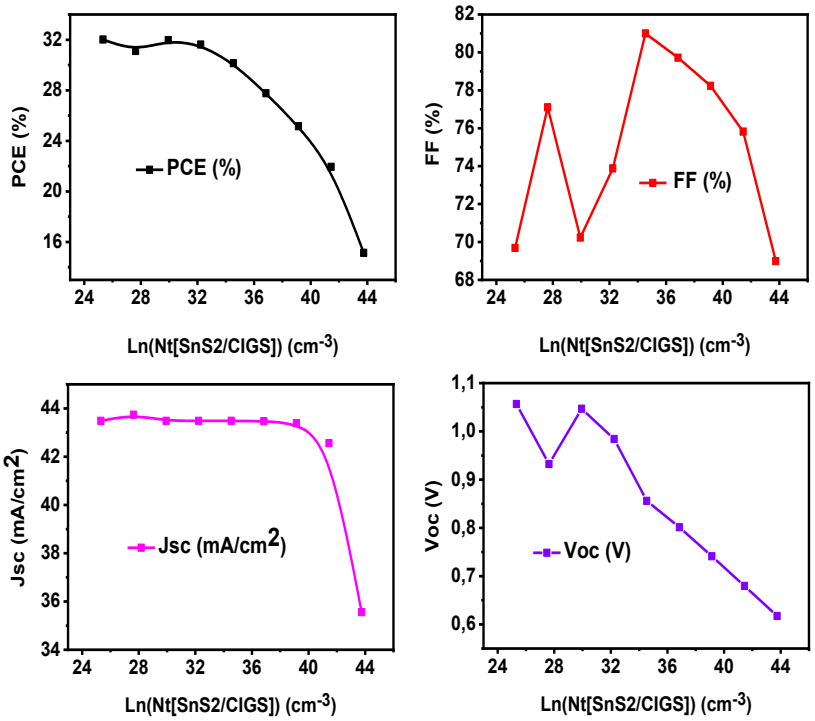

Figure 10: The influence of interfacial defect density (Nt) at the SnO2/CIGS hetero-junction on the key photovoltaic parameters of the CIGS solar cell.

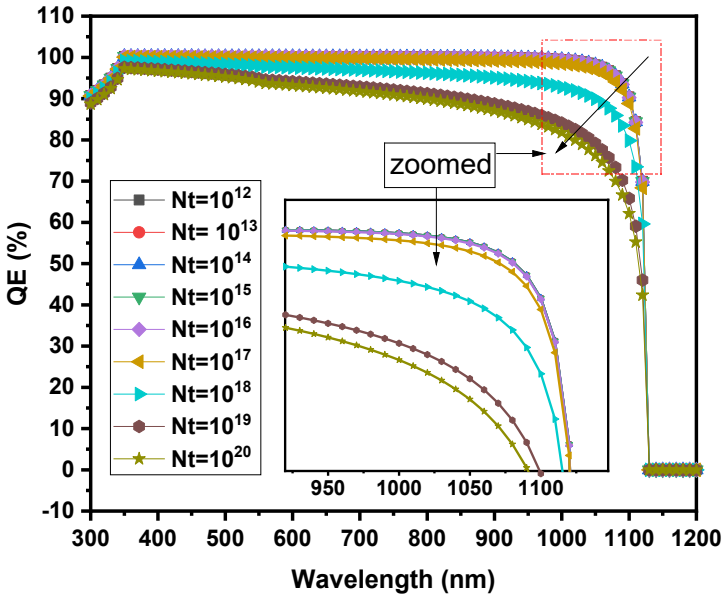

Figure 11: Varaiation of quantum efficiency with interfacial defect density (Nt) at the SnS2/CIGS hetero-junction on the key photovoltaic parameters of the CIGS solar cell.

Journal of Information Systems Engineering and Management
2026, 11(1s)
e-ISSN: 2468-4376
https://www.jisem-journal.com/

Research Article

With the increase in defect density, the recombination of carriers also increases owing to the decrease in various parameters. The simulation results reveal that at very low interfacial defect densities (e.g., 10^{12} cm^{-2}), the solar cell maintains high performance, with power conversion efficiency (PCE) values between 31.44% and 32.02%, high fill factors (FF) exceeding 69%, and short-circuit current densities (Isc) around 43.5 mA/cm^2. The open-circuit voltage (Voc) peaks at 1.0566 V at 10^{10} cm^{-2}, indicating minimal recombination losses at the interface. However, as Nt increases beyond 10^{13} cm^{-2}, a steady decline in Voc and efficiency is observed. For example, at 1014 cm^{-2}, Voc decreases to 0.8559 V, and efficiency drops to 30.15%. This degradation becomes more pronounced at higher defect densities. By 10^{18} cm^{-2}, Voc falls to just 0.6173 V, Isc drops significantly to 35.56 mA/cm^2, and efficiency declines to 15.14%. These trends are attributed to the increasing number of interface states that act as recombination centers. High interfacial Nt increases carrier recombination at the heterojunction, degrading the built-in potential, reducing carrier lifetime, and ultimately limiting both Voc and Isc. Despite FF values remaining relatively stable across most Nt levels, their contribution is not sufficient to compensate for the decline in voltage and current. Therefore, maintaining low defect densities at the SnSe2/CIGS interface is critical for high-efficiency device performance. The results suggest that optimal interfacial defect densities should be kept below 10^{13} cm^{-2} to minimize recombination losses and preserve photovoltaic performance.

Effect of Interfacial Defect Density at the CIGS/CBTS Interface on Solar Cell Performance

At very low defect densities (10^{12} cm^{-2}), the solar cell shows excellent performance. Power conversion efficiency (PCE) remains nearly constant at ~31.97–31.98%, with a high short-circuit current density (Isc ≈ 43.49 mA/cm^2), and an open-circuit voltage (Voc) of about 1.048 V. The fill factor (FF) is also stable around 70%, indicating minimal losses due to recombination at the heterointerface. As the interfacial defect density increases to 10^{13} cm^{-2} and above, a gradual degradation in performance is observed. Voc begins to decrease steadily from 1.034 V at 10^{13} cm^{-2} to just 0.7754 V at 10^{18} cm^{-2}. This decline in voltage reflects enhanced non-radiative recombination via interfacial trap states, which impairs the built-in potential at the junction. Despite FF increasing slightly at moderate Nt (reaching a maximum of 81.59% at 10^{15} cm^{-2}), the corresponding drop in Voc and Isc outweighs this benefit. At high defect densities (e.g., 10^{18} cm^{-2}), Isc decreases to 38.92 mA/cm^2, leading to a marked reduction in efficiency down to 24.02%. These results clearly demonstrate that the CIGS/CBTS interface must be carefully engineered to minimize interfacial defect states. Maintaining Nt below 10^{13} cm^{-3} is critical for preserving high Voc and overall device efficiency. Excessive interfacial defects lead to significant recombination losses, confirming the interface as a limiting factor in device optimization.

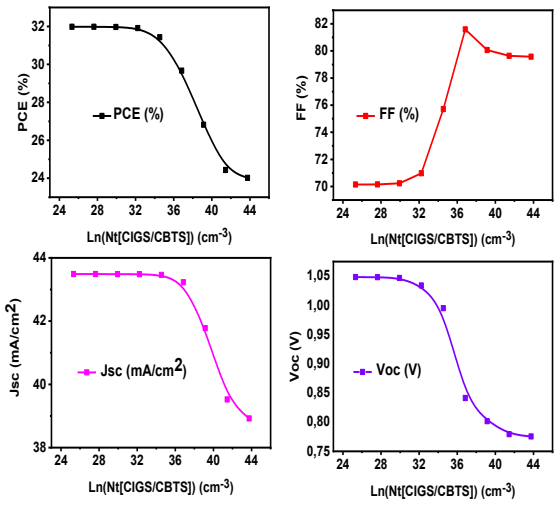

Figure 11: The influence of interfacial defect density (Nt) at the CIGS/CBTS interface on solar cell characteristics.

Journal of Information Systems Engineering and Management
2026, 11(1s)
e-ISSN: 2468-4376
https://www.jisem-journal.com/

Research Article

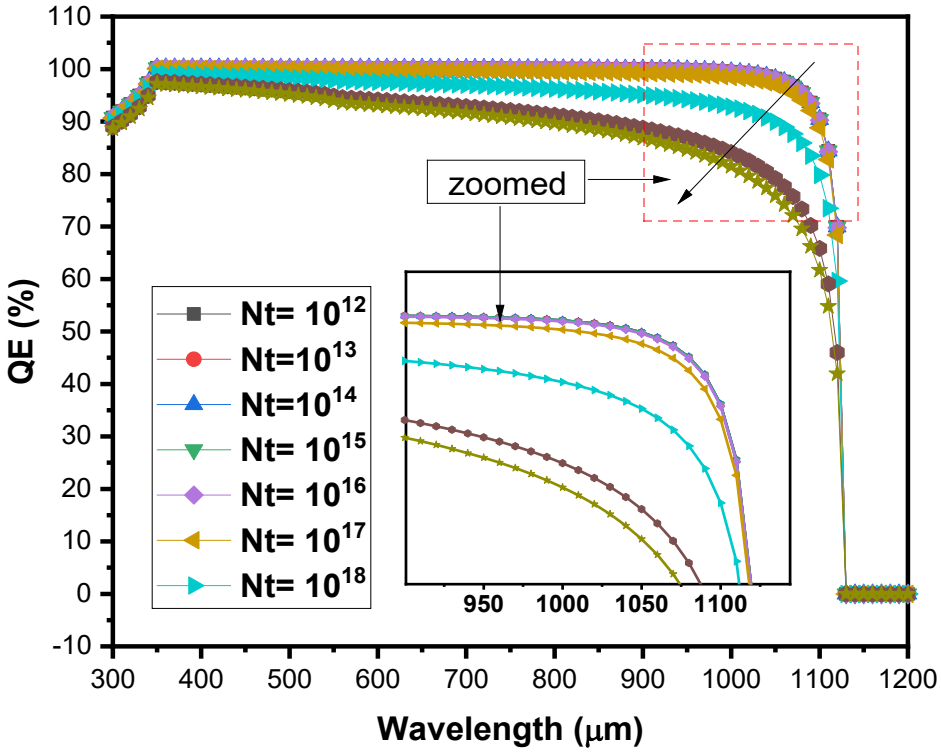

Figure 13: Variation of quantum efficiency with interfacial defect density (Nt) at the CBTS/CIGS hetero-junction on the key photovoltaic parameters of the CIGS solar cell.

OPTIMIZED CIGS SOLAR CELL STRUCTURE

In the following the optimized CIGS solar cell structure with ETL using SnSe2 material and CBTS as a BSF layer (see **Figure 14**). **Table 4** resume the optimum physical values of optimized CIGS solar cell such as Na, Nt and D.

Table 4 The optimized values for each studied parameter.

Parameters	ETL	BSF	Na (CIGS)	Nt (CIGS)	Nt (CIGS/CBTS)	Nt (SnS2/CIGS)	D (CIGS)
Optimized values	SnSe2	CBTS	10^{18} cm^{-3}	10^{14} cm^{-3}	10^{13} cm^{-3}	10^{13} cm^{-3}	1 µm

Journal of Information Systems Engineering and Management
2026, 11(1s)
e-ISSN: 2468-4376
https://www.jisem-journal.c

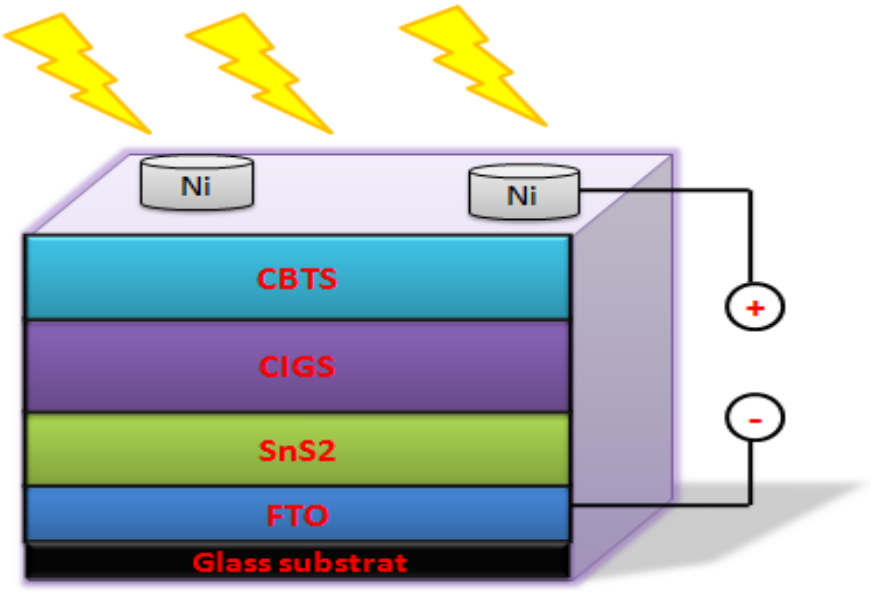

Figure 11: Illustration of efficient CIGS solar cell with optimized ETL/BSF layers.

According the previous investigation of BSF and ETL layers effect on the performance of solar cell, several candidate BSF materials including CBTS, CuSbS2, AgInTe2, CuSCN, MoSe2, Sb2S3, and Sb2Se3 were suggested, also four ETL layers were tested including SnS2,. ZrS2, CdS and WS2 but the best combination was obtained for CBTS and SnS2. Additionally, after the optimization of thickness, doping concentration (Na) and defects density (Nt) in CIGS layer. The results demonstrated that the CIGS/CBTS and SnS2/CIGS interfaces must be below 10^{13} cm^{-3} for preserving high Voc and overall device efficiency. The optimized parameters were tabulated in **Table 4**.

CONCLUSION

This study presents a comprehensive simulation-based optimization of CIGS (Cu(In,Ga)Se2) solar cells, focusing on the effects of various Electron Transport Layer (ETL) and Back Surface Field (BSF) material combinations. The SnS2/CBTS configuration emerged as the top-performing architecture, achieving a peak efficiency of 31.44%, with excellent short-circuits current and voltage characteristics. Additional parametric studies evaluated the effects of absorber layer thickness, doping concentration (NA), and defect densities (bulk and interfacial) on device performance. Results indicate that an absorber thickness of 1 μm, an optimal doping level of 10^{18} cm^{-3}, and minimal defect densities ($\leq 10^{13}$ cm^{-3}) are crucial for maximizing efficiency. Quantum efficiency (QE) analysis confirmed enhanced spectral response for the optimized structure. The results clearly demonstrated that the CIGS/CBTS and SnS2/CIGS interfaces must be carefully engineered to minimize interfacial defect states. Maintaining Nt below 10^{13} cm^{-3} is critical for preserving high Voc and overall device efficiency.

ACKNOWLEDGMENTS

The researchers wish to extend their sincere gratitude to the Deanship of Scientific Research at the Islamic University of Madinah (KSA) for the support provided to the Post-Publishing Program.

CONFLICTOFINTEREST

The authors declare no conflict of interest.

REFRENCES

[1] Zhu, L., et al. (2018). Piezo-phototronic and pyro-phototronic effects to enhance Cu(In, Ga)Se2 thin-film solar cells. Energy & Environmental Science, 11(7), 3877–3885.

[2] Tian, S.-S., et al. (2024). Design of back-contact interface of Cu(In, Ga)Se2 solar cells by single-target magnetron sputtering. Acta Physica Sinica, 73(17).

[3] Monnaf, M. A., et al. (2025). The development and evaluation of hybrid solar cells based on perovskites and

CIGS with different ETL for increased photovoltaic efficiency using SCAPS-1D. Langmuir, 41(20), 12556–12576.

[4] Burgelman, M., et al. (2000). Modelling polycrystalline semiconductor solar cells. *Thin Solid Films, 361*, 527–532.

[5] Ram Mohan Reddy Kundavaram, Rahul Reddy Bandhela, Abhishake Reddy Onteddu. (2022). AI-Driven Predictive Modeling In Healthcare: A Data Science Perspective On U.S. Healthcare Data. South Eastern European Journal of Public Health. https://doi.org/10.70135/seejph.vi.6691

[6] Bhattarai, S., et al. (2021). Numerical simulation study for efficiency enhancement of doubly graded perovskite solar cell. *Solar Energy, 118*, 111285.

[7] Bhattarai, S., & Das, T. (2021). Optimization of carrier transport materials for performance enhancement of the MAGeI2-based perovskite solar cell. *Solar Energy, 217*, 200–207.

[8] Schock, H.-W. (1993). CuInSe2 and other chalcopyrite-based solar cells. *MRS Bulletin, 18*(10), 42–44.

[9] Oyedele, S. O., Soucase, B. M., & Aka, B. (2016). Numerical simulation and performance optimization of Cu(In, Ga)Se2 solar cells. *International Journal of Applied Physics, 18*(1).

[10] Valencia, D., et al. (2021). Optimization of Cu(In, Ga)Se2 (CIGSe) thin film solar cells parameters through numerical simulation and experimental study. *Solar Energy Materials & Solar Cells, 224*, 298–308.

[11] Grandell, L., & Höök, M. (2015). Assessing rare metal availability challenges for solar energy technologies. *Sustainability, 7*(9), 11818–11837.

[12] Chadel, M., et al. (2023). Enhancement in efficiency of CIGS solar cell by using a p-Si BSF layer. *Materials, 16*(7), 2956.

[13] Rahman, M. F., et al. (2024). Improving the efficiency of a CIGS solar cell to above 31% with Sb_2S_3 as a new BSF: A numerical simulation approach using SCAPS-1D. *RSC Advances, 14*(3), 1924–1938.

[14] Meusel, M., et al. (2002). Spectral mismatch correction and spectrometric characterization of monolithic III–V multi-junction solar cells. *Solar Energy Materials & Solar Cells, 10*(4), 243–255.

[15] Seaman, C. H. (1982). Calibration of solar cells by the reference cell method — The spectral mismatch problem. *Solar Energy, 29*(4), 291–298.

[16] Oublal, E., et al. (2022). High performance of a new solar cell based on carbon nanotubes with CBTS compound as BSF using SCAPS-1D software. *Journal of Nano Research, 24*(10), 202.

[17] Djatoubai, E., & Su, J. (2021). First spray pyrolysis thin-film fabrication of environment-friendly Cu_2BaSnS_4 (CBTS) nanomaterials. *Chemical Physics Letters, 770*, 138406.

[18] Del Cueto, J. (1998). Method for analyzing series resistance and diode quality factors from field data of photovoltaic modules. *Solar Energy Materials & Solar Cells, 55*(3), 291–297.

[19] Del Cueto, J. (1999). Method for analyzing series resistance and diode quality factors from field data — Part II: Applications to crystalline silicon. *Solar Energy Materials & Solar Cells, 59*(4), 393–405.

[20] Sylla, A., et al. (2021). Theoretical analysis of the effect of the interfacial MoSe2 layer in CIGS-based solar cells. *Energy Reports, 9*(4), 339–350.

[21] Asaduzzaman, et al. (2016). An investigation into the effects of band gap and doping concentration on Cu(In, Ga)Se2 solar cell efficiency. *SpringerPlus, 5*(1), 578.

[22] Ghavami, F., & Salehi, A. (2020). High-efficiency CIGS solar cell by optimization of doping concentration, thickness, and energy band gap. *Modern Physics Letters B, 34*(04), 2050053.

[23] Kamikawa, Y., et al. (2025). Highly efficient lightweight flexible Cu(In, Ga)Se2 solar cells with a narrow bandgap fabricated on polyimide substrates: Impact of Ag alloying, Cs and Na doping, and front shallow Ga grading on cell performance. *Advanced Energy Materials, 5*(2), 2400404.

[24] Benchiheb, N., et al. (2024). Emitter thickness and solar cell efficiency: The role of deep-level defects and Auger recombination. In *Proceedings of the 3rd International Conference on Advanced Electrical Engineering (ICAEE)*. IEEE.

[25] Dimitrijev, S. (2006). Principles of semiconductor devices. *IEEE Circuits and Devices Magazine, 22*(5), 58–59.

[26] Cheng, S. (2024). High-efficiency wide gap Cu(In, Ga)Se2 solar cells: Influence of buffer layer characteristics. heliyon, 10(17).